

PROCEEDINGS OF SPIE

[SPIDigitalLibrary.org/conference-proceedings-of-spie](https://spiedigitallibrary.org/conference-proceedings-of-spie)

Phase retrieval method for multiple wavelength speckle patterns

Petrov, Nickolay, Bespalov, Victor, Gorodetsky, Andrei

Nickolay V. Petrov, Victor G. Bespalov, Andrei A. Gorodetsky, "Phase retrieval method for multiple wavelength speckle patterns," Proc. SPIE 7387, Speckle 2010: Optical Metrology, 73871T (13 September 2010); doi: 10.1117/12.871433

SPIE.

Event: Speckle 2010, 2010, Florianapolis, Brazil

Phase Retrieval Method for Multiple Wavelength Speckle Patterns

Nickolay V. Petrov, Victor G. Bespalov, Andrei A. Gorodetsky

Department of Photonics and Optical Informatics, St. Petersburg State University of Information Technology, Mechanics and Optics, 199004, Kadetskaya Linia 3, St. Petersburg, Russia;

ABSTRACT

We present a wavefront retrieval method for radiation comprising several wavelengths. Both numerical models and experimental results are presented. Numerical modeling implies iterative phase retrieval procedure for all wavelengths in spectrum. For reconstruction we can use two different algorithms, one inherits from one proposed by Osten, Pedrini and Almoró, the second one implies expansion by Hermite-Gauss or Laguerre-Gauss basis set which allows to decrease calculation time consumption. In experiment, speckle patterns can be formed either by spectral supercontinuum radiation from photonic-crystal fiber (PCF) or by Stokes components of stimulated Raman scattering (SRS) from second harmonic of pulse Nd:YAG laser radiation in barium nitrate crystal.

Keywords: phase retrieval, image reconstruction, speckle, diffraction theory

1. INTRODUCTION

Two different approaches for wavefront retrieval are known so far. The first one is a holographic method that uses reference source to register interference pattern that could be reconstructed afterwards, nowadays it is often replaced by digital holography methods. We should mention methods with virtual reference beam,¹ when full object diffraction field is reconstructed from registered intensity by creating higher frequency quasi-periodic modulation with carrying interference lines on a registered speckle structure, which imitates holographic recording.

The second approach expunges use of reference beam in any way and uses iteration procedure for retrieval of lost in intensity pattern phase instead. Development of computation speed stimulates growth in research and publication in this topic.^{2,3} For example, Pedrini and Osten^{4,5} suggested single-beam multiple-intensity reconstruction, (SBMIR) as a method for referenceless phase retrieval. This method uses images of various parts of volume speckle fields and wave propagation equation. As shown in⁴ SBMIR-technology is a perspective method for wavefront retrieval because it implies using of rustic experimental setup. In comparison with other phase retrieval techniques, such as Gerchberg-Saxton(GS) and Yang-Gu(YG) algorithms, that have constraint that the test object is known to be either a phase-only or an amplitude only, SBMIR-technology can be used both for amplitude and/or amplitude-phase objects both in transmission and reflection ways.

In this paper, we propose similar method of referenceless wavefront reconstruction involving multiple wavelength speckle patterns. Wave propagation equation can be used as one describing wavefront variation due to wavelength change from λ_1 to λ_2 at a fixed distance l . Within the framework of this approximation the possibility for combining this technique with SBMIR is shown. Use of three RGB wavelengths radiation, corresponding to spectral response of CCD matrix and DCRaw image converter, allowing to extract the spectral information from Bayer filter channels in documental mode with extended dynamic range,⁶ yields three diffraction patterns from one exposure which is well enough for full wavefront retrieval.

In the first part the algorithm and some derivations that can be used in calculations are described. In the second part light sources and setup design are discussed. In the third section computational modeling and experimental results are given. In the last part the conclusion is presented.

Further author information: Send correspondence to Nickolay Petrov, E-mail: Nickolai.Petrov@gmail.com

2. ITERATION ALGORITHM AND WAVE PROPAGATION EQUATIONS

Wavefront retrieval method from several speckle patterns is similar to SBMIR and acts as follows: Reconstruction process starts from wavelength which amplitude is derived by square root taking from first intensity distribution. Then this amplitude is multiplied to phase (constant for the first iteration) that yields a wave field in this plane. For this function (wave field complex function) object plane wave field was reconstructed (which obviously differs from an object at initial iterations). Reconstructed wave field in the object plane was used for calculation of second speckle pattern (calculated for the next wavelength in suggested method and at a different distance in SBMIR). In the computed field we drop the amplitude and substitute it with a square root of the second registered speckle pattern intensity. Then, the same operation as in the first step is performed, namely, the field resulting from modeled propagation phase and measured intensity square root as an amplitude is propagated back to object plane and used as a start field for the next iteration. When the measured intensities are over, we go to first one again and repeat the procedure.

Two dimensional Fresnel transform can be used for paraxial wave propagation modeling:

$$F(x, y, l) = \frac{k}{2\pi il} \iint_{\mathbb{R}^2} \exp\left(\frac{ik}{2l}[(x-x')^2 + (y-y')^2]\right) F_0(x', y') dx' dy'. \quad (1)$$

here $F(x, y, l)$ is a complex function; x, y — coordinates at a plane; l — propagation variable; $F_0(x', y') = F(x, y, 0)$; $k = 2\pi/\lambda$.

As it was already mentioned, Fresnel transform could be used as an equation, describing wavefront alteration due to wavelength change from λ_1 to λ_2 at its propagation to fixed distance l .⁷ To make it obvious, the following change of variables is necessary: Let $\lambda_2 = m\lambda_1$. Then to prevent a change in wave propagation equation we should replace the distance as follows $l_2 = l_1/m$. This replacement will be correct only if we deal with flat objects, where phase incursion could be neglected. If a volume structure is used, one should perform derivations involving phase incursion carefully. Furthermore, for accurate reconstruction of grayscale objects, equality in radiation energies is necessary, i.e. in fact all spectral components should be justified to be equal in terms of power.

There is another point to be made here that described technique can use not only two dimensional Fresnel transform as light propagation equation. Rayleigh-Sommerfeld equation or expansion in basic Hermite-Gauss(2) or Laguerre-Gauss(3) functions set can be used instead:

$$\mathcal{H}_{n,m}(x, y) = \exp(-x^2 - y^2) H_n(\sqrt{2}x) H_m(\sqrt{2}y), \quad (n, m = 0, 1, \dots), \quad (2)$$

$$\mathcal{L}_{n,\pm m}(x, y) = \exp(-x^2 - y^2) (x \pm iy)^m L_n^m(2x^2 + 2y^2), \quad (n, m = 0, 1, \dots). \quad (3)$$

here $H_n(t) = (-1)^n e^{t^2} \frac{d^n}{dt^n} (e^{-t^2})$, $L_n^m(t) = \frac{1}{n!} t^{-m} e^t \frac{d^n}{dt^n} (t^{n+m} e^{-t})$.

— are Hermite and Laguerre polynomials correspondingly. This function sets are invariant under Fresnel transform:^{8,9}

$$\mathcal{H}_{n,m}(x, y, l) = \frac{1}{|\sigma|} \exp\left(\frac{2il(x^2 + y^2)}{kW_0^4|\sigma|^2} - i(n+m+1)\arg\sigma\right) \mathcal{H}_{n,m}\left(\frac{x}{W_0|\sigma|}, \frac{y}{W_0|\sigma|}\right), \quad (4)$$

$$\mathcal{L}_{n,\pm m}(x, y, l) = \frac{1}{|\sigma|} \exp\left(\frac{2il(x^2 + y^2)}{kW_0^4|\sigma|^2} - i(2n \pm m + 1)\arg\sigma\right) \mathcal{L}_{n,\pm m}\left(\frac{x}{W_0|\sigma|}, \frac{y}{W_0|\sigma|}\right). \quad (5)$$

where $\sigma = 1 + \frac{2il}{kW_0^2}$ — is a complex parameter used for more compact representation, $W_0 = \text{const}$ — is a Gauss beam width. It would be effective to choose W_0 to be comparable with minimal elements on a transparent object.

As this functions are orthogonal and complete in $L_2(\mathbb{R}^2)$, they can serve as a basis and expanding $F_0(x, y)$ function at $l = 0$, we can write down it easily for any other l . Theoretically, there's no difference between all

basic function sets, however, as cartesian coordinate system is used by default, Hermite-Gauss functions are more convenient in use, because they have corresponding symmetry. Expansion for this basis will be as follows :

$$F_0(x, y) = \sum_{n=0}^{\infty} \sum_{m=0}^{\infty} c_{nm} \mathcal{H}_{n,m}(x, y, 0), \quad c_{nm} = \frac{1}{\|\mathcal{H}_{n,m}\|^2} \iint_{\mathbb{R}^2} F_0(x, y) \mathcal{H}_{n,m}(x, y, 0) dx dy, \quad (6)$$

$$F(x, y, l) = \sum_{n=0}^{\infty} \sum_{m=0}^{\infty} c_{nm} \mathcal{H}_{n,m}(x, y, l) \quad (7)$$

Substituting $\mathcal{H}_{n,m}(x, y, l)$ from (4) to (7) we get:

$$F(x, y, l) = \frac{1}{|\sigma|} \exp\left(\frac{2il(x^2 + y^2)}{kW_0^4|\sigma|^2}\right) \sum_{n=0}^{\infty} \sum_{m=0}^{\infty} c_{nm} \exp(-i(n+m+1)\arg\sigma) \mathcal{H}_{n,m}\left(\frac{x}{W_0|\sigma|}, \frac{y}{W_0|\sigma|}\right). \quad (8)$$

For (8), as it was already performed for Fresnel transform, we can exchange variables $l_2 = l_1/m$ and describe wavefront alterations that will occur at changing wavelength from λ_1 to $\lambda_2 = m\lambda_1$ at its propagation to distance l_1 .

Processing speed of the proposed algorithm using basis Hermite-Gauss functions depends basically on object transparency function and parameter W_0 . However, this method has its advantages when numerical focusing is performed,⁴ when basis expanded wavefront can be virtually propagated to any distance by recalculating coefficients in (8) and by scaling $\mathcal{H}_{n,m}$ functions only.

3. LIGHT SOURCES

One can use various sources of light for suggested technique. At design stage some of light sources were tested to fit, such as spectral components of supercontinuum, stokes components of SRS from pulse Nd:YAG laser second harmonic generated on barium nitrate crystal. High monochromaticity is the essential requirement for light source for this method as spectral components of broadband radiation smudge the diffraction pattern. For such light sources as spectral supercontinuum generator, fiber Bragg grating can be used for separation of spectral components. In case of Stokes SRS components from second Nd:YAG harmonic, spectral components can be split with beam splitters and mirrors in optical scheme.

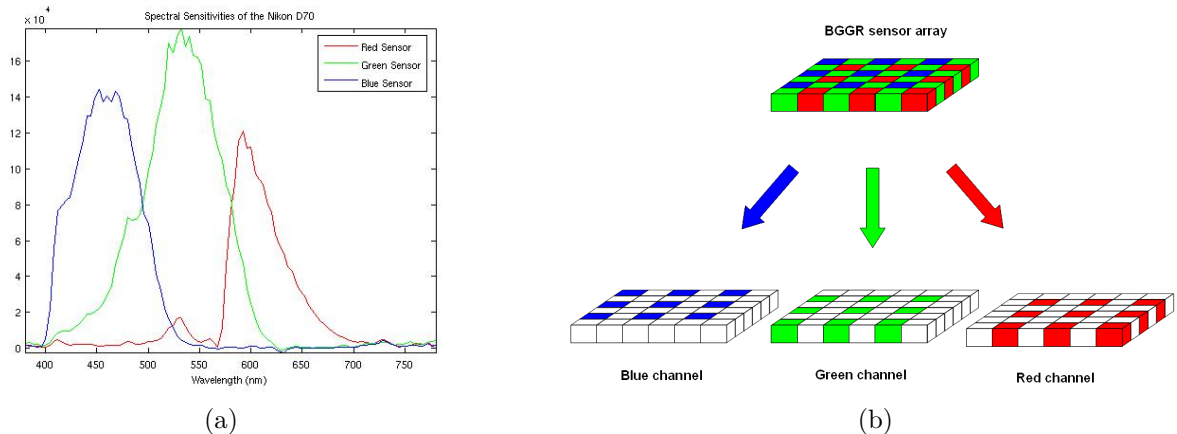


Figure 1. (a) — Spectral response of CCD Nikon D70/D50; (b) — Bayer BGGR array (top), divided into RGB channels (bottom).

One of the main advantages of this method in compare to SBMIR, is the possibility to register up to three diffraction speckle patterns at one shot. Figure 1 (a) shows spectral response of NikonD70/D50 camera CCD array. Selecting narrow spectral components, corresponding to maximal sensitivity for each of three color CCD channels we can implement the described technique. Experimentally it was performed for two color channels at a

time — both for $R + G$ and $R + B$, because green channel of Nikon D50 used for this experiment has rather high sensitivity at second harmonic of Nd:YAG laser used ($532nm$) as well as at blue light from DPSS laser ($473nm$). Anyway, available combinations allowed to retrieve wavefront. Shooting was save to RAW format (used for separate R, G and B channels registration), processing started from extraction of spectral components from RAW image with DCRaw converter with parameters `-4 -T -D *.NEF`. These parameters convert 12 bit camera ADC data to 16 bit Tiff file without either any color interpolation, usually performed by camera processor or scaling. Afterwards, data array in BGGR format (see Fig.1(b)) (or RGGB) is divided into three arrays corresponding to three RGB channels, pixel size in each of new arrays being twice bigger than original.

4. NUMERICAL SIMULATION AND EXPERIMENT

4.1 Numerical Simulation

As an example here we present a diffraction pattern from amplitude transparent letter **A** obtained using 2D Fresnel transform (Fig.2 (a)) and using Hermite-Gauss expansion as well (Fig.2 (b, c)). As it is obviously seen from figures, when correct parameters (W_0 , and Hermite-Gauss functions number) are taken, close agreement between methods can be reached.

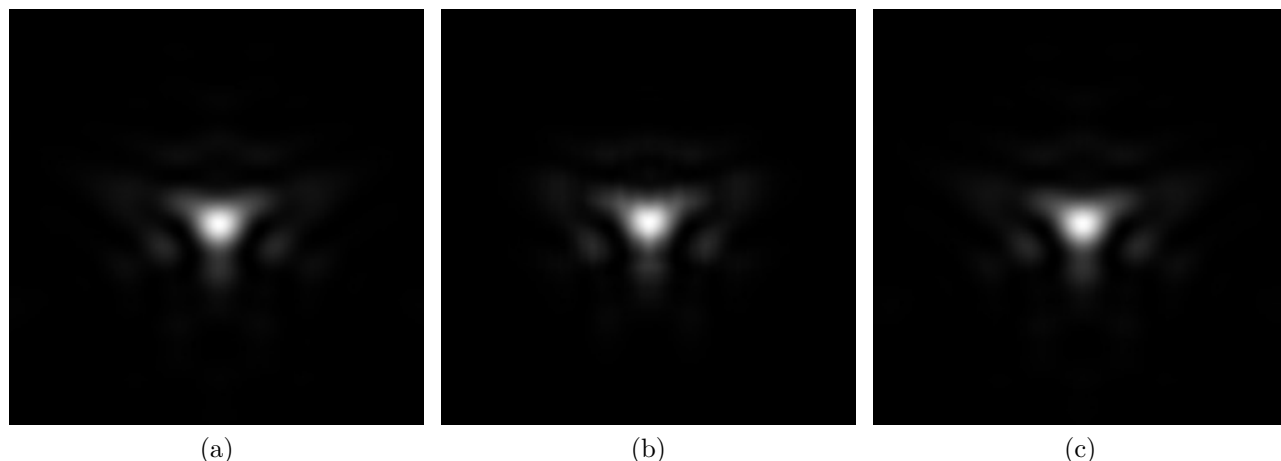


Figure 2. Two wave propagation models comparison (a) — Diffraction pattern obtained using 2D Fresnel transform; (b) — Diffraction pattern obtained using Hermite-Gauss expansion, relative normal error to (a) = 0.053; (c) — Diffraction pattern obtained using Hermite-Gauss expansion, relative normal error to (a) = 0.02

In these paper, presented results are obtained using Fresnel transform as a wavefront propagation equation. Double Fresnel integral is calculated by successive nonrecurrent integration. Integration area was divided into pixels, followed by using Gauss method with an order(number of points per pixel) of 1 to 3. At a PC with 2GHz CPU and 2Gb RAM one iteration involving processing of 3 diffraction patterns (800×800 pixels) took about 30 seconds.

During simulation, algorithm convergence was tested both for amplitude and phase objects, and amplitude-phase objects as well. Generally, convergence is proportional to number of speckle pattern shots used, but is also depends on other parameters, such as spatial/spectral distance between shots, number of points in object and image etc. Optimum number of various speckle patterns for reconstruction turned to be more than six, however, it should be noticed here that alignment errors, that will obviously occur in real experiment can negatively affect the reconstruction and grow with number of shots.

In conclusion, we can tell that modelling results are in good agreement with previous research.⁴

4.2 Experiment

In our experimental setup we used 3 lasers with different wavelengths and beam splitters (Fig. 3).

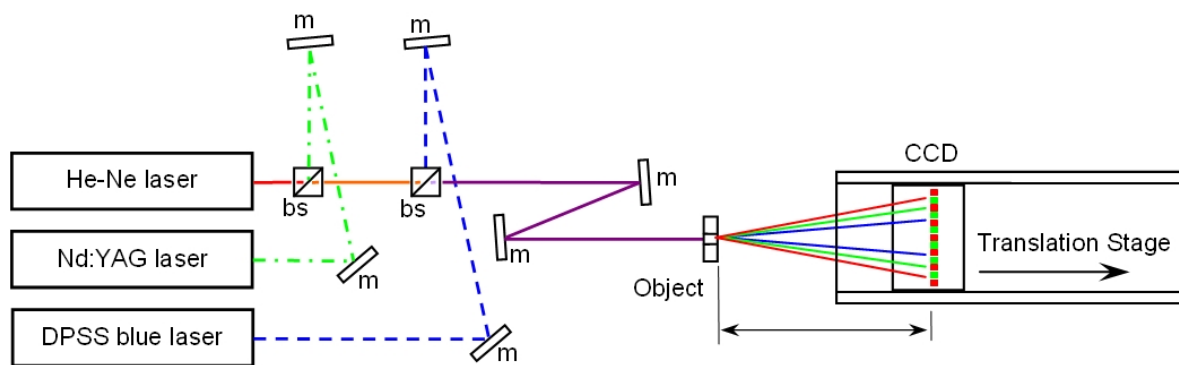


Figure 3. Scheme of experimental setup. Each laser beam was scattered on an object put into diaphragm after passing two mirrors *m* and beam splitters *bs*. Registration was performed on a Nikon D50 camera CCD array.

For three-color diffraction pattern the following lasers were used: He-Ne laser (632.8 nm), Nd:YAG laser (1064 nm and its second harmonic 532 nm), and DPSS laser (473 nm). As an amplitude object an **A** letter image on a microfilming film stuck onto a diaphragm is used. Height of the letter is about 430 μm . Diffraction patterns are registered by digital Nikon D50 camera without a lens (2014×3039 pixels 7.8 μm each) into RAW format with further RGB channel information extraction in documental mode with extended dynamic range. In experiment, both consequent and simultaneous registration of different wavelengths are tested (Fig. 4).

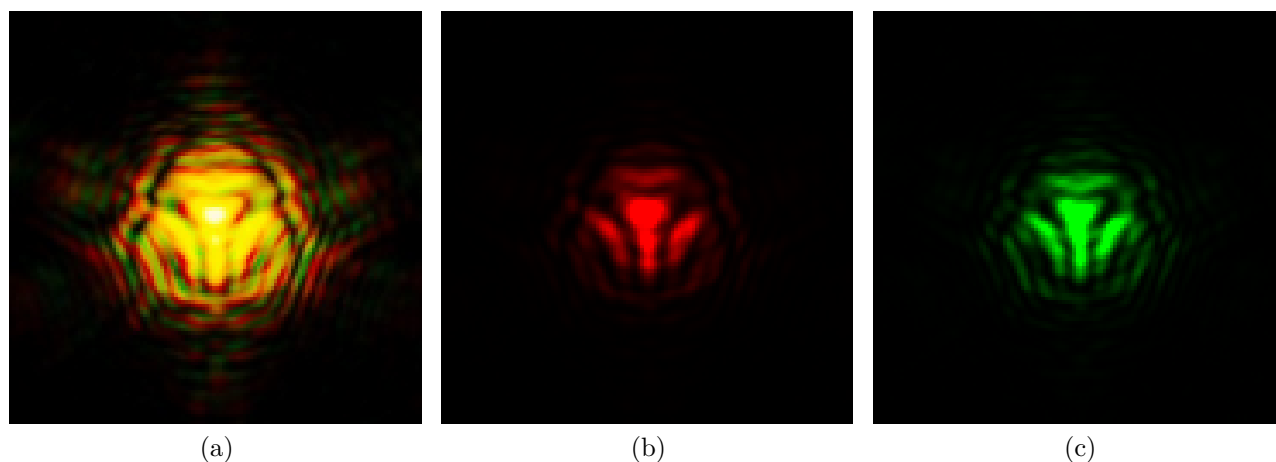


Figure 4. Diffraction interference patterns of He-Ne and Nd:YAG second harmonic radiation recorded at one exposure (a) in both spectral channels; (b) — Red; (c) — Green.

Use of single-coordinate motorized translation stage from Standa allowed to register interference diffraction patterns from all wavelengths at various distances to use them jointly in iteration algorithm.

Previously mentioned normalization of each wavelength radiation power is very essential. In case of binary object like the one we use here improper normalization won't affect much, but for grayscale object this action is crucial. In our experiment the object actually is a grayscale due to insufficient microfilm density (Fig. 5 (a)) but normalization wasn't performed, that results in more distinguishable gray background in single-wavelength reconstruction (Fig. 5 (b)),

Still, principal convergence of proposed method may be considered as proven (Fig. 5 (c))

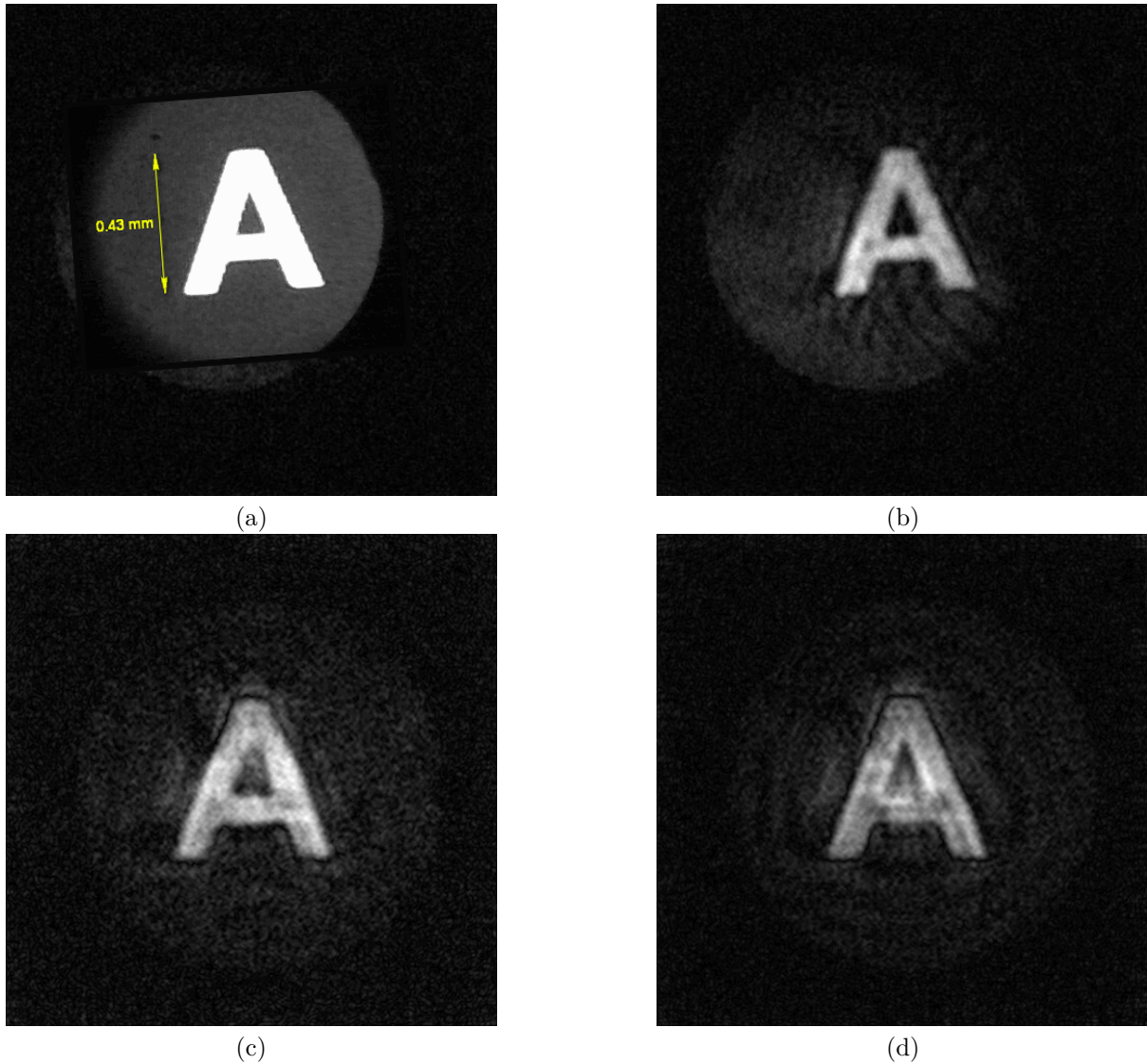


Figure 5. Image of the object used in experiment (a) — made through microscope; (b) — experimentally reconstructed from amplitude object diffraction patterns registered at various distances; (c) — experimentally reconstructed from amplitude object diffraction patterns of three different wavelengths; (d) — experimentally reconstructed from amplitude object diffraction patterns of three different wavelengths registered at two different distances (6 speckle patterns altogether).

Addition of new patterns registered with the same wavelengths but at other distances allows to improve accuracy of reconstruction, despite the affect of experimental error growth, the result of such addition can be seen in Fig. 5 (d) — lines in letter **A** became more smooth, the reason for bad grayscale reconstruction has already been discussed.

5. CONCLUSION

A new method for wavefront reconstruction after diffraction on amplitude, phase and amplitude-phase transparents by means of numerical simulation is presented.

Experimental reconstruction of amplitude object printed on microfilming film wavefront using several wavelength diffraction patterns is presented.

In this paper, a competitive technique of wavefront retrieval from speckle patterns set is presented. Combination of multi-color speckle patterns with speckle patterns at several distance can also be used for reconstruction.

Further work involves experiments with other light sources and careful accounting of experimental parameters and errors.

6. ACKNOWLEDGEMENTS

The work was supported by St.Petersburg Government Grant (in 2008 and 2009).

REFERENCES

1. B. B. Gorbatenko, L. A. Maksimova, and V. P. Ryabukho, "Reconstruction of the hologram structure from a digitally recorded fourier specklegram," *Opt. Spect.* **106**(2), pp. 1562–6911, 2009.
2. J. A. Rodrigo, H. Duadi, T. Alieva, and Z. Zalevsky, "Multi-stage phase retrieval algorithm based upon the gyrator transform," *Opt. Express* **18**, pp. 1510–1520, 2010.
3. L. Camacho, V. Mico, Z. Zalevsky, and J. Garcia, "Quantitative phase microscopy using defocusing by means of a spatial light modulator," *Opt. Express* **18**, pp. 6755–6766, 2010.
4. P. Almoró, G. Pedrini, and W. Osten, "Complete wavefront reconstruction using sequential intensity measurements of a volume speckle field," *Appl. Opt.* **45**, pp. 8596–8605, 2006.
5. Y. Zhang, G. Pedrini, W. Osten, and H. Tiziani, "Whole optical wave field reconstruction from double or multi in-line holograms by phase retrieval algorithm," *Opt. Express* **11**, pp. 3234–3241, 2003.
6. M. Konnik, E. Manykin, and S. Starikov, "Increasing linear dynamic range of commercial digital photocamera used in imaging systems with optical coding," in *Proceedings of OSAV Topical meeting*, (Saint-Petersburg, Russia), 2008.
7. R. Collier, C. Burckhardt, and L. Lin, *Optical Holography*, New York; London: Academic Press, 1971.
8. E. G. Abramochkin, "Hermite-laguerre-gaussian functions," *Vestnik Samara State Univ.* **4**(22), p. 19, 2001.
9. V. A. Soifer, *Computer Optics Methods*, Fizmatlit, Moscow, 2003.